Retinal microvascular features are associated with CMR measures of subclinical cardiovascular dysfunction

Cian Wade[1], Alicja R Rudnicka[2], Hana El Diwany[3], Charlotte Zheng[3], Ian Yeung[3], Robin D Hamilton[3], Masliza Mahmod[4,5], Helena B Thomaides Brears[5], Charlie Diamond[5], Ravi Pattanshetty[5], John Anderson[6], Ryan Chambers[6], Roshan A Welikala[7], Jiri Fajtl[7], Sarah A Barman[7], Elijah R Behr[1], Christopher G Owen[2]

Corresponding author:

Dr Cian Wade MD, MA, MPH, MRCP
cwade@citystgeorges.ac.uk

Cardiovascular and Genomics Research Institute,
City St George's, University of London,
Cranmer Terrace,
London,
SW17 0RE

[1]Cardiovascular and Genomics Research Institute, City St George's, University of London, London, UK; [2]Population Health Research Institute, City St George's, University of London, London, UK; [3]Moorfields Eye Hospital NHS Foundation Trust, London, UK; [4]Division of Cardiovascular Medicine, Radcliffe Department of Medicine, University of Oxford, Oxford, UK; [5]Perspectum Ltd., Oxford, UK; [6]Homerton Healthcare NHS Foundation Trust, London, UK; [7]Kingston University, London, UK

Abstract

Background

Microvascular dysfunction is a key component of many cardiovascular (CV) diseases. Assessing the retinal microvasculature through retinal imaging may therefore provide a window into evaluating a range of CV diseases. This study sought to generate hypotheses regarding relationships between different retinal microvascular features (RVF) and measures of subclinical CV dysfunction derived from cardiovascular magnetic resonance (CMR) imaging.

Methods

182 participants with type 2 diabetes enrolled in the UK Imaging Diabetes Study (UKIDS) with CMR image data were considered for inclusion in this cross-sectional study. Fifteen CMR measures of cardiac structure, function, tissue characterisation, adiposity, and aortic distensibility were derived. One-hundred-twenty-eight participants (70%) were found to have eligible retinal images. An artificial intelligence (AI)-enabled retinal imaging analysis tool (QUARTZ) quantified eight RVFs from each participant's retinal image: arteriolar and venular diameter, area, calibre uniformity, and tortuosity. Correlation analysis shortlisted RVF-CMR variable pairs for multivariable regression. Regression coefficients represent change per 1 standard deviation (SD) increase in RVF.

Results

Sixteen RVF-CMR regression pairs were shortlisted for regression, and five remained associated after adjustment for potential confounders. Per 1-SD increase in venular tortuosity was associated with a 0.5ms greater left ventricular (LV) T2 mean, 0.6% worsening in LV global longitudinal strain, and a 2 mL greater left atrial max volume. Per 1-SD increase in arteriolar calibre uniformity and retinal venular area were associated with 9ms lower LV T1

mean and $0.2x10^{-3}mmHg^{-1}$ greater proximal descending aortic distensibility respectively. No significant associations were found between RVF and LV volumetric or functional measures, or adiposity.

Conclusions

In a diabetic cohort, we identified novel and biologically plausible associations between RVF and CMR measures of subclinical CV dysfunction. This provides new insight into the relationship between the retinal and systemic vascular beds and supports the potential role of retinal imaging in evaluating CV dysfunction prior to onset of overt disease.

Introduction

Features of the retinal microvasculature are predictive of a range of cardiovascular (CV) diseases[1,2]. This has heightened interest in the utility of retinal imaging as a non-invasive and scalable method of population health screening for CV disease[3]. The retinal microvasculature encompasses a variety of geometric features of the retinal arteriolar and venular beds. Numerous prospective studies have demonstrated an association between narrower arteriolar diameters with coronary heart disease, hypertension, and heart failure[2,4,5]. Conversely, wider venular diameter is associated with incident stroke and smaller venular branching angle associated with worse left ventricular (LV) function[6,7]. Retinal microvascular features encompassing diameter, tortuosity, and area are predictive of myocardial infarction and stroke [1].

Beyond associations with clinically apparent, or overt, CV disease, evidence is emerging of the relationship between the retinal microvasculature and indicators of subclinical CV dysfunction prior to onset of overt disease. Changes in arteriolar geometric features, including vessel branching angles and tortuosity are related to echocardiographic features of maladaptive cardiac remodelling such as increased LV diameter, LV mass and left atrial (LA) volume index[8]. Optical Coherence Tomography angiography demonstrates that lower capillary density is associated with hypertension-related LV remodelling including higher mass, interstitial volume and worsened longitudinal strain[9]. Early features of macrovascular disease such as arterial and aortic stiffness are associated with narrower retinal arteriolar diameter[10,11,12].

Cardiovascular magnetic resonance (CMR) imaging is the gold-standard technique for characterisation of many of these often subclinical CV abnormalities[13]. However, CMR is currently not a point of care test, despite availability in secondary care and imaging centre

settings. Moreover, patients with subclinical disease will not routinely be referred for CMR, limiting its utility for diagnosing and monitoring early CV disease. This contrasts with the relative accessibility and low-cost of retinal imaging, with the majority of these images acquired in the community as part of routine eye-checks. The case for using retinal imaging as a tool for evaluating CV disease rests on the retinal microvasculature providing a readily accessible window into systemic vascular health[14]. Microvascular dysfunction is a hallmark of many CV diseases, frequently preceding and also occurring in parallel to macrovascular CV disease[15,16,17]. The mechanistic link between retinal and systemic vascular beds is their shared susceptibility to systemic factors, including inflammatory mediators and haemodynamics[18,19]. This likely explains why retinal microvascular changes contribute their own independent risk to adverse CV outcomes[20,1,4,6].

The present study sought to further explore associations between the retinal microvasculature and CMR measures of cardiac structure, function, tissue characterisation, adiposity, and aortic distensibility. We performed an exploratory cross-sectional observational study in a cohort of patients with type 2 diabetes who had undergone both retinal and CMR imaging as part of the UK Imaging Diabetes Study (UKIDS). Utilising AI-enabled retinal image analysis, we examined the relationship between participants' retinal microvascular features (RVF) and CMR measures. The objective was to generate hypotheses regarding relationships between the retinal microvasculature and subclinical features of CV dysfunction.

Methods

Study design

The UK Imaging Diabetes Study (UKIDS, clinical trial registration number: NCT05057403) is an ongoing real-world, multi-centre prospective cohort study with clinical outcome collection of individuals with type 2 diabetes and without a recent history of incident CV disease. UKIDS participants were considered for inclusion who had been recruited from Moorfields Eye Hospital NHS Foundation Trust in London, UK, between June 2022 – September 2025. All participants had type 2 diabetes and were having regular outpatient retinal monitoring as part of their routine diabetic management. Exclusion criteria were evidence of incident CV event(s) within 12 months prior to consent, including myocardial infarction, unstable angina, heart surgery, ischaemic stroke, and transient ischaemic attack. Other exclusion criteria included known liver disease, known significant renal tract abnormalities, alcohol dependency, and contraindication to MR scanning.

CMR data collection & processing

All participants underwent a standardised multi-organ multiparametric MR scan (CoverScan™; Perspectum, Oxford) on a 3T scanner at the Alliance Medical Imaging Centre, London, UK[21]. Acquired CMR images were processed by trained radiographers and MR technologists blinded to clinical data. The following CMR measures were derived: left ventricle ejection fraction (LVEF); LV end diastolic volume indexed to body surface area (BSA) (LVEDVi); LV end systolic volume BSA (LVESVi); LV stroke volume BSA (LVSVi), LA max volume BSA (LAVi) LV mass BSA (LVMi), LV wall thickness (LVWT), LV T1 and T2 mean relaxation times averaged across all 16 American Heart Association (AHA) myocardial segments derived from the three short-axis views excluding the apex, LV

global longitudinal strain (LV GLS), LV global circumferential strain (LV GCS), LV global radial strain (LV GRS), epicardial adipose tissue (EAT), pericardial adipose tissue (PAT), and aortic distensibility measures (supplementary table 1). Data were centrally curated and quality-controlled. A cardiologist accredited to European Association of Cardiovascular Imaging level 3 for CMR independently reviewed all cardiac scans. Where pathology was identified, consensus was sought from a second independent cardiologist with this same accreditation. Scans were reviewed to exclude regional wall motion abnormalities, clinically significant valvular abnormalities, and other cardiac pathology. If a given CMR measure had a reporting completion of <70% across included participants, then this measure was not included in the analysis. Demographic and self-reported clinical information were collected from participants by UKIDS researchers during a face-to-face consultation prior to CMR images acquisition (supplementary table 2).

Retinal image collection & processing

We searched for a single macular centred retinal image of either eye for these 182 participants on imaging databases held at Moorfields Eye Hospital NHS Foundation Trust and the North East London Diabetic Eye Screening programme with the following selection criteria applied: colour fundus image of either eye captured with a 45° field of view; retinal image captured within a 2-year period either before or after the date the CMR images were acquired; quality of retinal image ≥70% (as per QUARTZ methodology outlined below). Where multiple retinal images met the inclusion criteria, the image with quality ≥90% was selected; if more than one image had quality ≥90%, the image closest to the CMR date was selected. If multiple images met the inclusion criteria but none had quality ≥90% (all were 70-89%), then the image closest to the CMR date was selected. One retinal image was ultimately selected per participant for subsequent analysis.

A fully-automated artificial intelligence (AI)-enabled system (QUARTZ)[22] was applied to extract and quantify thousands of measures related to the retinal microvasculature within each single retinal image. QUARTZ uses deep learning to classify retinal vessels as an arteriole or venule, map the optic disc, and calculate an image quality score ranging from 0-100%. For this study, eight RVF measures were used from QUARTZ's output: arteriolar and venular diameter (µm), area (mm^2), calibre uniformity (1/µm), and tortuosity (arbitrary units). We define vessel calibre uniformity as the variability of the diameter of vessels within an individual's retina. This is calculated by the median standard deviation of vessel diameter along vessel segments, computed per image and inverted to normalise. Therefore, greater vessel calibre uniformity indicates lower variability of diameter, and vice-versa. Pixels from each retinal image were converted to physical units (in microns) using the QUARTZ output of the optic disc vertical diameter as a calibration reference standard[23]. RVF diameter, calibre uniformity, and tortuosity were calculated for each identified vessel and an average (weighted by length of the vessel segment) calculated for each participant's image. RVF area represents the total arteriolar or venular area in each image.

Statistics

Statistical analysis was carried out using Stata (StataCorp LLC. Stata Statistical Software: Release 19.5. College Station (TX); 2024). See supplementary table 3 for additional details on statistical methods. Participant demographic and clinical characteristics were reported, as well as RVF and CMR measure mean and standard deviation (where normally distributed) or median and interquartile range (where non-normally distributed). A participant was excluded from further analysis if any RVF or CMR measure had a |z| score >4, to minimise the influence of potentially artefactual retinal vessel or CMR measurements.

Exploratory Pearson's correlation was performed by examining matrices and scatter plots of 120 RVF and CMR pairs. These included all 8 RVFs paired with all CMR measures that met ≥70% reporting completion but excluded volumetric measures that were not indexed to BSA. For each RVF-CMR pair, participants with missing data for the CMR measure were excluded from that correlation analysis. To address multiple testing, we applied a multi-step selection strategy to shortlist RVF-CMR pairs for further regression analysis. First, we required associations to demonstrate both a minimum effect size ($|r| \geq 0.15$) and statistical significance ($p<0.05$). These thresholds are justified given the exploratory, hypothesis-generating objective of this study. Second, we evaluated the biological feasibility of relationships meeting this threshold.

Prior to regression analysis, we assessed normality assumptions using the Shapiro-Wilk test, skewness, and kurtosis. Where violations were identified, we attempted log transformation and applied robust standard errors where violations persisted (supplementary table 3a). Additionally, systolic blood pressure (SBP) was unrecorded among 16 (12.5%) participants at the time of CMR imaging. We performed a Missing at Random (MAR) assessment of any systematic differences in demographic, clinical, RVF and CMR variables between participants where SBP was recorded versus missing (supplementary table 3b). We then proceeded with multiple imputation by chained equations with predictive mean matching for handling missing SBP data (supplementary table 3c).

We performed multivariable linear regression on the multiply imputed datasets to predict CMR measures from RVF. Where a CMR measure was missing for the measure under analysis, participants were dropped from the regression models without imputation. We hypothesised that age at CMR, sex, SBP, duration of type 2 diabetes, and time between retinal and CMR images could confound the relationship between RVF and CMR measures. We therefore included each of these potential confounders as covariates in sequential models

1-6 (supplementary table 4). Model 6 included a centre-specific fixed effects (α_j) to account for potential variation in retinal image acquisition processes between the different retinal imaging centres participants attended (supplementary table 3d). Regression coefficients are reported as both unstandardized (β represents change in CMR measure units per 1 standard deviation [SD] increase in RVF) and standardized (βSD represents change in SD units of CMR measure per 1-SD increase in RVF), along with p-values for these estimates with statistical significance set at $\alpha=0.05$. 95% confidence intervals are reported and correspond to the main β or βSD estimate. Finally, sensitivity analysis was performed to assess the stability of β regression coefficient estimates to reduced sample size (supplementary table 3e).

Ethics

Informed written consent was obtained from all study participants enrolling in the UKIDS trial. Ethical approval for UKIDS was provided by the West Midlands – Solihull research ethics committee (ethics reference 20/WM/0007). Retinal imaging data used from the North East London Diabetic Eye Screening programme was approved by NHS Health Research Authority and Health and Care Research Wales (Integrated Research Application System number 265637). This study was conducted in accordance with the Declaration of Helsinki. Anonymised individual patient data can be shared upon request or as required by law and/or regulation with qualified external researchers. Approval of such requests is at the discretion of the study sponsors and is dependent on the nature of the request, the availability of the data, and the intended use of the data.

Results

Demographic & clinical characteristics

182 participants in the UKIDS study recruited from Moorfields Eye Hospital NHS Foundation Trust underwent CMR imaging between June 2022 and September 2025. 129 (71%) of these had retinal images which met the inclusion criteria. One participant (0.8%) was excluded due to extreme RVF measurements (venular diameter Z=4.2, arteriolar area Z=7.8, venular area Z=8.4), indicating likely imaging artefact. Therefore, 128 participants (70%) were included for analysis (Figure 1). No systematic demographic, RVF or CMR differences were observed between the 128 included and 54 excluded participants. Of the included participants, 88 (69%) were male, 40 (31%) were female and their mean age was 62 years (SD 9) (Table 1). 37% were of White ethnic origin, 32% South Asian, 23% Black, and 8% from other groups. Mean duration of type 2 diabetes was 17 years (SD 9), with mean SBP of 138mmHg (SD 17), diastolic blood pressure of 79mmHg (SD 9), and mean BMI of 29 kg/m² (SD 5). 8% were current smokers, 22% past smokers, and 70% had never smoked. 68% of patients had a known diagnosis of hypertension. Previous CV events were rare (5% myocardial infarction, 5% stroke, 2% angina, 0% heart failure), with all events occurring >12 months prior to recruitment.

Figure 1: Participant flow diagram

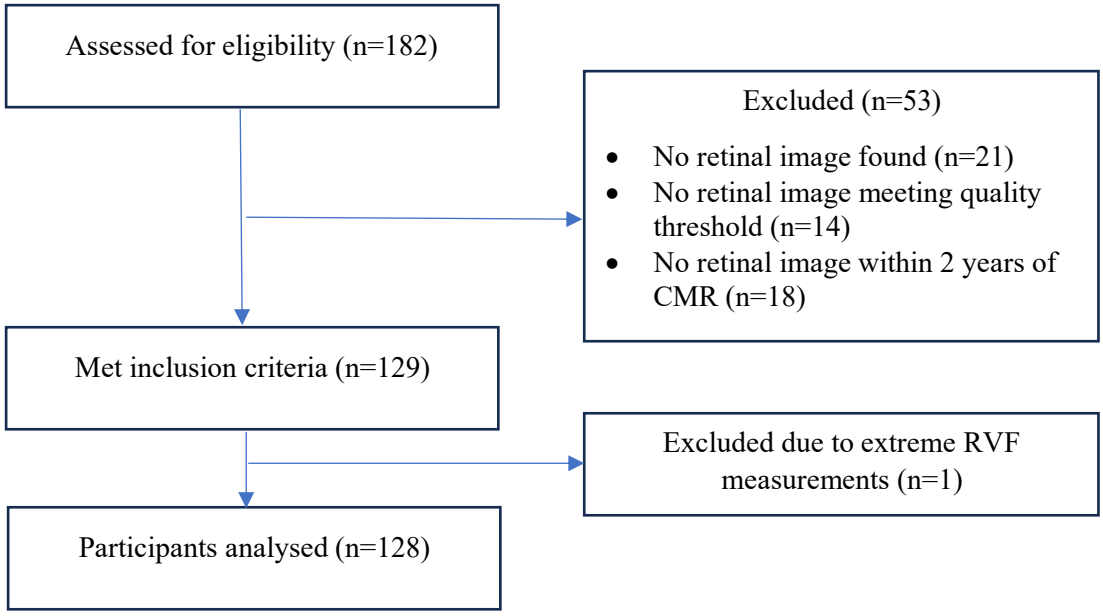

Table 1: Baseline characteristics of included participants

Mean (SD) unless otherwise stated

Demographic characteristics	**Value**
Participants included (n)	128
Age[1] (years)	62 (9)
Sex (n, % male)	88 (69%)
Ethnicity (%, n participants)	
White	37% (47)
South Asian	32% (40)
Black	23% (29)
Other	8% (10)
Clinical characteristics	
Duration of type 2 diabetes[1] years	17 (9)
Days between CMR and retinal image	179 (192)
Systolic blood pressure mmHg	138 (17)
Diastolic blood pressure mmHg	79 (9)
BMI (kg/m²)	29 (5)
Current smoker	8% (10)
Past smoker	22% (28)
Never smoker	70% (70%)
CV disease history (%, n participants)	
Hypertension	68% (87)
Myocardial infarction	5% (7)
Stroke	5% (7)
Angina	2% (3)
Heart failure	0% (0)
Retinal vessel feature	
Arteriolar diameter (μm)	77.3 (11.9)
Venular diameter (μm)	81.4 (13.6)
Arteriolar area (mm^2)	4.2 (1.3)
Venular area (mm^2)	4.6 (1.7)
Arteriolar calibre uniformity (1/μm)	0.1 (0.03)
Venular calibre uniformity (1/μm)	0.1 (0.03)
Arteriolar tortuosity (arbitrary units)	1.2 (0.4)
Venular tortuosity (arbitrary units)	1.4 (0.3)
CMR measure	
LV ejection fraction (%)	58 (6)
LV end diastolic volume BSA (mL/m^2)	70 (14)
LV end systolic volume BSA (mL/m^2)	30 (8)
LV stroke volume BSA (mL/m^2)	40 (8)
LA max volume BSA (mL/m^2)	27 (10)
LV mass BSA (g/m^2) (Median, IQR)	49 [43 – 55]
LV wall thickness (mm)	12 (2)
LV T1 mean (ms)	1213 (35)
LV T2 mean (ms)	39 (2)
LV global longitudinal strain (%) (Median, IQR)	-16 [-18 , -15]
LV global circumferential strain (%)	-17 (3)
LV global radial strain (%) (Median, IQR)	28 [24 – 31]
Epicardial adipose tissue (cm^2)	11 (3)
Pericardial adipose tissue (cm^2)	26 (13)
Proximal descending aortic distensibility ($x10^{-3}mmHg^{-1}$) (Median, IQR)	1.5 [1.0 – 2.1]

IQR: Interquartile range; BMI: Body mass index; BSA: Body surface area; [1]Referenced to date of CMR; Ethnicity % relates to the 126 participants where ethnicity was recorded; BP was recorded in 112, BMI in 125, all other measures recorded in all 128 participants

CMR and RVF baseline characteristics

Fifteen CMR measures met the threshold of ≥70% reporting completeness and were included for further analysis (table 1; CMR measure reference values in supplementary table 5). LV function and volumes were consistent with preserved systolic function (LVEF 58%, LVESVi 30 mL/m^2, and LVSVi 40mL/m^2). Normal LVEDVi (70mL/m^2), LVMi (49g/m^2), LAVi (27mL/m^2) and high-normal LVWT (12mm) indicated there was no evidence of adverse chamber remodelling.

Mean LV T1 (1213ms) and T2 (39ms) signals averaged across 16 AHA segments were within a normal range. LV GLS (-16%) and LV GCS (-17%) were mildly impaired, while LV GRS (median 28%) was normal. Mean EAT (11cm^2) and PAT area (26cm^2) were normal. Mean proximal descending aortic distensibility (PDAoD) was reduced (1.5 x10^{-3}mmHg^{-1}), consistent with increased arterial stiffness observed in diabetes[24].

RVF measures derived from QUARTZ were calculated (table 1). Arteriolar diameter (77.3μm) and area (4.2mm^2) were smaller than venular diameter (81.4μm) and area (4.6mm^2). This directionality between the arteriolar and venular measures is consistent with previously published QUARTZ derived data on these measures[10,25]. Arteriolar calibre uniformity (0.1 1/μm) and venular calibre uniformity (0.1 1/μm) were comparable. Tortuosity was lower among arterioles (1.2) than venules (1.4), consistent in magnitude with prior published data[24].

Correlation analysis

Correlation analysis was performed for the 8 RVF measures against 15 CMR measures, yielding 120 pairwise correlations (supplementary table 6). LV mean T1 and T2 were significantly correlated with a variety of RVF measures. Lower values of T1 were correlated with greater arteriolar (r=-0.25, p=0.006) and venular calibre uniformity (r=-0.21, p=0.021). Higher values of T1 (r=0.19, p=0.04) and T2 (r=0.25, p=0.005) were correlated with greater venular tortuosity. Impaired LV GLS (less negative values) correlated with greater venular tortuosity (r=0.19, p=0.047). This was the only statistically significant relationship found between RVF and myocardial strain parameters. PDAoD was positively correlated with both arteriolar (r=0.28, p=0.008) and venular area (r=0.25, p=0.017), as well as with venular calibre uniformity (r=0.24, p=0.027). LAVi was the only volumetric parameter significantly correlated with an RVF measure (venular tortuosity, r=0.21, p=0.022). EAT area was positively correlated with arteriolar tortuosity (r=0.19, p=0.046) and PAT area negatively correlated with venular tortuosity (r=-0.20, p=0.031).

Overall, 15 RVF-CMR pairs reached the inclusion threshold of $|r| \geq 0.15$ and $p<0.05$. Correlations not reaching this threshold included those between RVF measures and LVEF, LVEDVi, LVESVi, LVSVi, LVMi, LVWT, and LV GCS and LV GRS. While the correlation between venular tortuosity and PAT area met threshold for inclusion, the negative directionality was considered to lack biological plausibility and was therefore excluded from subsequent regression analysis. A further two pairs were selected for regression due to borderline statistical significance and biological plausibility of a potential relationship (venular area and LV GRS, r=0.18, p=0.052; and venular area and LVEF, r=0.15, p=0.097). This resulted in a final selection of 16 RVF-CMR pairs for further analysis with multivariable regression (table 2).

Model diagnostics and missing data

Model diagnostics revealed that residuals from three RVF-CMR pairs, all involving PDAoD, showed marginal normality violations, with robust standard errors subsequently used for regressions involving this outcome (supplementary table 7). The MAR assumption for multiple imputation was well supported with no systematic differences in baseline demographic, clinical, RVF, and CMR characteristics between groups with and without recorded SBP (supplementary table 8).

Multivariable regression

Five of the 16 RVF-CMR pairs revealed statistically significant associations in fully adjusted multivariable linear regression models (table 2). Venular tortuosity was the RVF most consistently associated with CMR measures. Each 1-SD increase in venular tortuosity was associated with a 1.9mL (95% confidence interval, 0.1 - 3.8mL) increase in LAVi, 0.6% (0.2 - 1.1%) worsening of LV GLS, and 0.5ms (0.1 - 0.8ms) increase in LV T2 mean. Each 1-SD increase in venular area was associated with a 0.2 $x10^{-3}mmHg^{-1}$ (0.02 - 0.4 $x10^{-3}mmHg^{-1}$) increase in PDAoD. Arteriolar calibre uniformity was the only non-venular RVF measure that had a statistically significant association with a CMR measure. Each 1-SD increase in arteriolar calibre uniformity was associated with an 8.8ms (-17.4 , - 0.2ms) decrease in LV T1 mean. No significant associations were found in regressions involving LVEF (with venular area, p=0.102) and EAT (with arteriolar tortuosity, p=0.331). Arteriolar diameter, venular calibre uniformity and arteriolar tortuosity were RVF predictors not found to be significantly associated with any of the outcome CMR variables. Changes in SD units of CMR measure per 1-SD increase in RVF (βSD) indicated a moderate magnitude of effect for the five significant associations (figure 2).

Relatively modest median changes in the β regression coefficient estimates were observed across all sequential models (supplementary table 9). We did not observe any change in the directionality of the associations across sequential models. By the final model 6, nine associations that were significant in the unadjusted model had lost significance, five retained significance and none of the initially non-significant pairs gained significance. Sensitivity analysis assessing coefficient stability under reduced sample size showed generally low coefficients of variation (median 19%), suggesting the primary significant associations identified through multivariable regression were robust (supplementary table 10).

Table 2: Correlation & fully adjusted regression models for the 16 RVF-CMR associations

		Correlation		Fully adjusted regression			
Predictor RVF variable	**Outcome CMR variable**	**r**	**p-value**	**β**	**β_{SD}**	**p-value**	**n**
Arteriolar diameter	LV T1 mean (ms)	0.19	0.041	5.6 (-0.91 - 12.17)	0.16	0.091	120
Arteriolar diameter	LV T2 mean (ms)	0.20	0.027	0.3 (-0.13 - 0.64)	0.11	0.197	123
Arteriolar area	PDAoD ($x10^{-3}mmHg^{1}$)	0.28	0.008	0.2 (-0.01 - 0.36)	0.18	0.057	89
Venular area	LVEF	0.15	0.097	0.9 (-0.18 - 1.96)	0.15	0.102	121
Venular area	LV GRS (%)	0.18	0.052	1.1 (-0.03 - 2.29)	0.17	0.056	114
Venular area	PDAoD ($x10^{-3}mmHg^{-1}$)	0.25	0.017	0.2 (0.02 - 0.38)*	0.19*	0.032	89
Arteriolar CU	LV T1 mean (ms)	-0.25	0.006	-8.8 (-17.35 , -0.21)*	-0.25*	0.045	120
Arteriolar CU	LV T2 mean (ms)	-0.25	0.006	-0.1 (-0.62 - 0.43)	-0.04	0.717	123
Venular CU	LV T1 mean (ms)	-0.21	0.021	-6.2 (-14.95 - 2.51)	-0.18	0.161	120
Venular CU	LV T2 mean (ms)	-0.28	0.002	-0.1 (-0.67 - 0.39)	-0.06	0.594	123
Venular CU	PDAoD ($x10^{-3}mmHg^{-1}$)	0.24	0.027	0.1 (-0.15 - 0.33)	0.09	0.462	89
Arteriolar tortuosity	EAT (cm^2)	0.19	0.046	0.3 (-0.33 - 0.97)	0.10	0.331	115
Venular tortuosity	LAVi (ml/m^2)	0.21	0.02	1.9 (0.07 - 3.78)*	0.20*	0.042	121
Venular tortuosity	LV T1 mean (ms)	0.19	0.042	5.9 (-0.19 - 12.02)	0.17	0.058	120
Venular tortuosity	LV T2 mean (ms)	0.25	0.005	0.5 (0.10 - 0.82)*	0.20*	0.013	123
Venular tortuosity	LV GLS (%)	0.19	0.047	0.6 (0.19 - 1.08)**	0.26**	0.006	114

β represents change in CMR measure units per 1 standard deviation [SD] increase in RVF in fully adjusted regression model 6; βSD represents the standard deviation change in the CMR measure per 1-SD increase in RVF in fully adjusted regression model 6; *p<0.05 **p<0.01

Figure 2: Standardised regression coefficient (βSD) for the 16 RVF-CMR associations in fully adjusted models

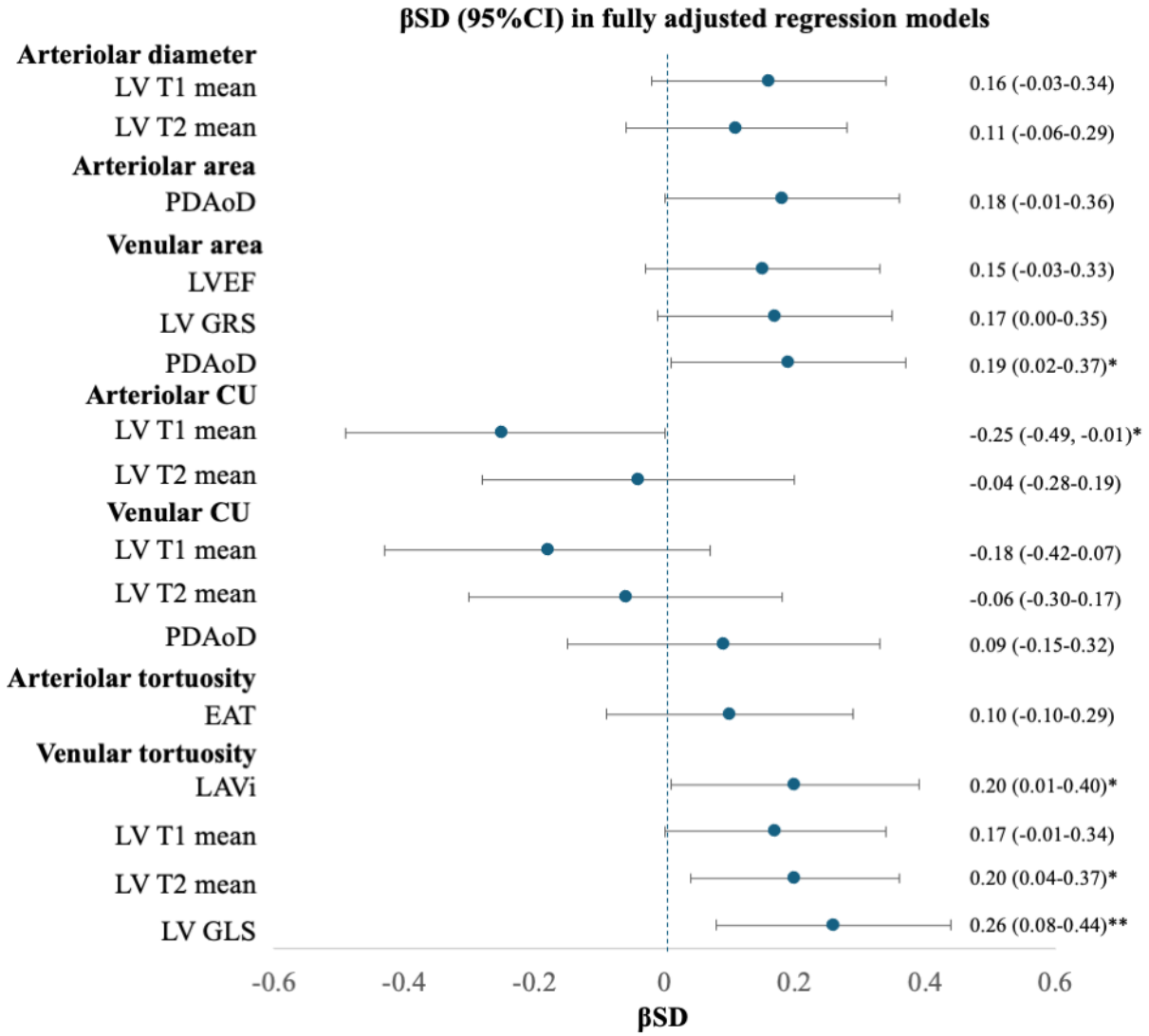

Forest plot demonstrates standardised regression coefficients (βSD) with 95% confidence intervals for the association between each RVF and CMR measure in the fully adjusted model 6. βSD represents the standard deviation change in the CMR measure per 1-SD increase in RVF in the fully adjusted model 6. Dashed vertical line represents the null (βSD=0); *p<0.05 **p<0.01

Discussion

In this cohort of patients with type 2 diabetes, we demonstrate a range of novel and biologically plausible associations between measures of the retinal microvasculature and subclinical features of CV dysfunction. To our knowledge, this is the first study to examine such a range of geometric retinal microvascular features against comprehensive CMR phenotypes.

Venular tortuosity was significantly associated with LV T2 mean, LV global longitudinal strain and left atrial volume. These CMR measures are consistent with a pattern of early diffuse myocardial dysfunction from low grade myocardial inflammation (increased T2), to subclinical impairment of LV contractility (less negative values of longitudinal strain) and atrial remodelling (increased LA volume)[26,27,28]. The biological plausibility of our findings is strengthened by the fact that this constellation of subclinical abnormalities is recognized to precede the development of overt heart failure syndromes[29]. Beyond venular tortuosity, we also noted that greater venular area was associated with increased proximal descending aortic distensibility and had a borderline association with better LV contractility (more positive values of radial strain). The directionality of these relationships aligns with previous findings that smaller retinal venular area is associated with an adverse cardiometabolic profile[30]. Overall, these associations support hypotheses that retinal venular abnormalities reflect microvascular pathology relevant to early CV disease[31]. While CV risk has traditionally focused on the arterial system, our findings suggest that the retinal venular bed also carries important information regarding CV dysfunction.

We also demonstrated associations between features of the retinal arteriolar bed and CMR measures. Greater arteriolar calibre uniformity was associated with lower LV T1 mean. This is biologically coherent and suggests that deranged retinal arteriolar morphology may reflect

broader systemic fibrotic processes, including myocardial fibrosis. We also observed a borderline association between greater arteriolar area and increases in proximal descending aortic distensibility. This aligns with recent work demonstrating a positive correlation between retinal arteriolar density and aortic distensibility[32], and reflects known shared pathophysiological links between the microvasculature and large arteries[33]. Together, these findings suggest that both the retinal arteriolar and venular beds can contribute to our understanding of distinct elements of subclinical CV dysfunction.

It is notable that we did not observe any significant relationships between LV functional or volumetric parameters and RVF measures. This may support the hypothesis that changes in RVF are primarily reflective of early microvascular dysfunction rather than downstream frank LV systolic or diastolic disease.

Notably, the literature remains inconsistent regarding which specific features of the retinal microvasculature are most associated with CV disease, and the directionality of these relationships. This can be partly attributed to high inter-study variability in the retinal imaging technique used, study cohorts, and methodological approaches to quantification of the retinal vascular tree. For example, our study found no evidence of a significant relationship between arteriolar and venular diameter and CMR measures. In contrast, these RVF measures have been central to previous work predicting CV disease[2,4,5]. It is possible that our sample size was under-powered to detect relationships between retinal microvascular diameter and CMR measures, which have been identified in larger cohorts. Another hypothesis is that arteriolar and venular diameter may manifest differently in diabetic patients compared with more clinically heterogenous groups[34]. This may also account for our cohort having a greater mean arteriolar and venular area than those seen in other studies[25]. Standardised imaging protocols and prospective studies in disease-specific cohorts will be important to future clinical translatability of retinal vascular imaging.

A key strength of this study is that we demonstrated that coefficient estimates were biologically plausible, directionally consistent, and relatively stable with use of multivariable regression models that accounted for several potential confounders. The likelihood that these significant associations (5 out of 16 associations) occurred by chance is extremely small (<1 in 1000). Another strength was the use of QUARTZ itself, which uses AI to extract a rich retinal vascular phenotype and has been extensively validated for use in large clinical and population-based studies[22]. The reproducibility and enhanced precision of RVF estimates derived from QUARTZ enabled more extensive and potentially reliable exploration of relationships with CMR measures than those reported in other studies. The characteristics of the study cohort were well suited to explore hypotheses regarding the relationship between RVF and subclinical CV dysfunction. While the cohort had no recent CV events, they all had type 2 diabetes, and a majority had hypertension. Chronic systemic inflammation associated with these two conditions may have increased the variance of RVF and CMR measures compared to a healthy cohort[35,18]. This greater range of subclinical microvascular phenotypes may have increased our ability to identify significant RVF-CMR relationships, while accounting for SBP and diabetes duration.

Limitations of this study include its small sample size, which meant that while this was an opportunistic exploratory study, we had limited power to detect several potentially true associations. Post-hoc power calculations indicate that with n=128 and α=0.05, our study had 80% power to detect correlations of $r \geq 0.25$, but lower power to detect smaller effects (r=0.10-0.20 corresponds to power of 20-62%). Sensitivity analysis with a ~10% reduction in sample size indicated that our five statistically significant associations had stable effect sizes and directionality, but significance was sometimes inconsistent across iterations. This highlights the need for a larger study to increase precision of effect size estimates, evaluate robustness of these findings, and determine the potential predictive utility of RVF measures. While this

diabetic cohort was appropriate for identifying subclinical cardiac dysfunction, further study should include healthy controls and those with established CV disease. This will test the generalisability of these findings and determine whether the observed associations are diabetes-specific or exist across the spectrum of CV health. Additionally, it is known that retinal vascular phenotype can vary between ethnic groups[36], and while we recruited a study cohort who were ethnically diverse, our sample size precluded meaningful stratified analysis by ethnicity. A further potential limitation is that absolute retinal vascular diameter, area, and calibre uniformity estimates require pixel-to-micron conversion using optic disc vertical diameter as a reference, meaning inter-individual variation in disc size may introduce measurement noise. Finally, this was a cross-sectional study where the CMR could occur before or after retinal image acquisition. Prospective studies will enable ascertainment of the temporality of the relationship between RVF and CMR measures and facilitate predictive inferences.

A key consideration is the clinical relevance of the magnitude of effect observed in several of the regression models. For the five associations found to be statistically significant we observed a moderate magnitude with a mean 0.21 SD change in CMR measure per 1-SD increase in RVF measure. This magnitude of effect is consistent with other epidemiological studies examining the relationship between CMR and demographic and clinical predictor variables such as age, sex, and diabetes status[37]. The modest absolute CMR measure unit changes associated with RVF measures likely reflect range restriction in our cohort without overt CV disease. In a cohort with established CV disease, where CMR measures would span a greater pathological range, larger and more clinically meaningful effect sizes would be anticipated. However, this may also point to best future clinical and public health use cases for retinal vascular imaging. It is less likely this technique would be deployed to finalise CV diagnoses, or guide treatment decisions where having sensitive measures of severity of

disease are critical. Ours and others' findings point more toward use cases in population health screening where identification of subclinical CV dysfunction can inform prioritisation of further diagnostic investigations, such as CMR or coronary angiography. Our findings also point towards a range of novel use cases beyond predicting atherosclerotic CV disease. These could include population health screening and identification of those at risk of aortic events, acquired or inherited cardiomyopathies, and poorly recognised diseases characterised by microvascular dysfunction such as heart failure with preserved ejection fraction (HFpEF)[38] and ischaemia with non-obstructed coronary arteries (INOCA)[39].

These findings demonstrate that features of the retinal microvasculature are associated with subclinical measures of CV dysfunction detected by CMR in patients with type 2 diabetes. Our study establishes a foundation for further investigation of these relationships with more directed study design in other patient cohorts. This will enable testing the predictive potential of RVF measures at different stages of CV disease processes and provide new mechanistic insights into the shared pathophysiology of micro- and macrovascular disease. Collectively, our findings strengthen the case for retinal imaging as a scalable and accessible method for detecting and evaluating early CV dysfunction.

Sources of funding

This study received no specific grant from any funding agency in the public, commercial or not-for-profit sectors. The UKIDS trial is sponsored by Perspectum Ltd. The sponsor was involved in data collection, analysis, and interpretation. Use of the North East London Diabetic Eye Screening programme data was funded by Wellcome Collaborative award (224390/Z/21/Z). CW's time was funded by the National Institute for Health and Care Research.

Disclosures

MM, HTB, CD, and RP are employees at Perspectum Ltd., the company that developed CoverScan™ used in this study, and funded recruitment of participants to the UKIDS trial. HTB is also a shareholder at Perspectum Ltd. ERB receives grant funding from The British Heart Foundation for projects unrelated to this study.

Author contributions

CW, ARR, IY, MM, and CGO conceptualised the study. Study methodology was developed by CW, ARR, RAW, JF, SAB, CGO. Investigation was conducted by HED, CZ, IY, RH, MM, HTB, CD, RP, JA, and RC. Formal analysis and interpretation were performed by CW and MM. The original manuscript was prepared by CW. All authors contributed to editing of the manuscript and approved the final version for submission. Supervision was provided by ARR, MM, ERB, and CGO. CW had full access to all data in the study and takes responsibility for their integrity and the accuracy of the data analysis.

References

[1] Rudnicka AR, Welikala RA, Barman SA, Foster PJ, Luben R, Hayat SA, Khaw KT, Whincup PH, Strachan DP, Owen CG. Artificial intelligence-enabled retinal vasculometry for prediction of circulatory mortality, myocardial infarction, and stroke. Br J Ophthalmol. 2022;106:1722–1729.

[2] Chandra A, Seidelmann SB, Claggett BL, Klein BEK, Klein R, Shah AM, Solomon SD. The association of retinal vessel calibres with heart failure and long-term alterations in cardiac structure and function: the Atherosclerosis Risk in Communities (ARIC) Study. Eur J Heart Fail. 2019;21:1207–1215.

[3] Hanssen H, Streese L, Vilser W. Retinal vessel diameters and function in cardiovascular risk and disease. Prog Retin Eye Res. 2022;91:101095.

[4] McGeechan K, Liew G, Macaskill P, Irwig L, Klein R, Sharrett AR, Klein BEK, Wang JJ, Chambless LE, Wong TY. Risk prediction of coronary heart disease based on retinal vascular calibre (from the Atherosclerosis Risk In Communities [ARIC] Study). Am J Cardiol. 2008;102:58–63.

[5] Wang JJ, Rochtchina E, Liew G, Tan AG, Wong TY, Leeder SR, Smith W, Shankar A, Mitchell P. The long-term relation among retinal arteriolar narrowing, blood pressure, and incident severe hypertension. Am J Epidemiol. 2008;168:80–88.

[6] McGeechan K, Liew G, Macaskill P, Irwig L, Klein R, Klein BEK, Wang JJ, Mitchell P, Vingerling JR, de Jong PTVM, et al. Prediction of incident stroke events based on retinal vessel calibre: a systematic review and individual-participant meta-analysis. Am J Epidemiol. 2009;170:1323–1332.

[7] Huang L, Chen WQ, Aris IM, Teo LLY, Wong TY, Koh AS, Li LJ. Associations between cardiac function and retinal microvascular geometry among Chinese adults. Sci Rep. 2020;10:14797.

[8] Huang L, Aris IM, Teo LLY, Wong TY, Chen WQ, Koh AS, Li LJ. Exploring associations between cardiac structure and retinal vascular geometry. J Am Heart Assoc. 2020;9:e014654.

[9] Chua J, Le TT, Sim YC, Chye HY, Tan B, Yao X, Wong D, Ang BWY, Toh DF, Lim H, et al. Relationship of quantitative retinal capillary network and myocardial remodeling in systemic hypertension. J Am Heart Assoc. 2022;11:e024226.

[10] Tapp RJ, Owen CG, Barman SA, Welikala RA, Foster PJ, Whincup PH, Strachan DP, Rudnicka AR. Associations of retinal microvascular diameters and tortuosity with blood pressure and arterial stiffness: United Kingdom Biobank. Hypertension. 2019;74:1383–1390.

[11] Lin F, Zhu P, Huang F, Li Q, Yuan Y, Gao Z, Yu P, Lin J, Chen F. Aortic stiffness is associated with the central retinal arteriolar equivalent and retinal vascular fractal dimension in a population along the southeastern coast of China. Hypertens Res. 2015;38:342–348.

[12] Cheung N, Sharrett AR, Klein R, Criqui MH, Islam FMA, Macura KJ, Cotch MF, Klein BEK, Wong TY. Aortic distensibility and retinal arteriolar narrowing: the multi-ethnic study of atherosclerosis. Hypertension. 2007;50:617–622.

[13] Salerno M, Sharif B, Arheden H, Kumar A, Axel L, Li D, Neubauer S. Recent advances in cardiovascular magnetic resonance: techniques and applications. Circ Cardiovasc Imaging. 2017;10:e003951.

[14] Liew G, Wang JJ, Mitchell P, Wong TY. Retinal vascular imaging: a new tool in microvascular disease research. Circ Cardiovasc Imaging. 2008;1:156–161.

[15] Orasanu G, Plutzky J. The pathologic continuum of diabetic vascular disease. J Am Coll Cardiol. 2009;53:S35–S42.

[16] Rehan R, Yong A, Ng M, Weaver J, Puranik R. Coronary microvascular dysfunction: a review of recent progress and clinical implications. Front Cardiovasc Med. 2023;10:1111721.

[17] Mohammedi K, Woodward M, Marre M, Colagiuri S, Cooper M, Harrap S, Mancia G, Poulter N, Williams B, Zoungas S, et al. Comparative effects of microvascular and macrovascular disease on the risk of major outcomes in patients with type 2 diabetes. Cardiovasc Diabetol. 2017;16:95.

[18] Cheung CY, Ikram MK, Klein R, Wong TY. The clinical implications of recent studies on the structure and function of the retinal microvasculature in diabetes. Diabetologia. 2015;58:871–885.

[19] Owen CG, Rudnicka AR, Welikala RA, Fraz MM, Barman SA, Luben R, Hayat SA, Khaw KT, Strachan DP, Whincup PH, et al. Retinal vasculometry associations with cardiometabolic risk factors in the European Prospective Investigation of Cancer-Norfolk Study. Ophthalmology. 2019;126:96–106.

[20] Wong TY, Klein R, Sharrett AR, Duncan BB, Couper DJ, Tielsch JM, Klein BEK, Hubbard LD. Retinal arteriolar narrowing and risk of coronary heart disease in men and women: the Atherosclerosis Risk in Communities Study. JAMA. 2002;287:1153–1159.

[21] Dennis A, Cuthbertson DJ, Wootton D, Crooks M, Gabbay M, Eichert N, Mouchti S, Pansini M, Roca-Fernandez A, Thomaides-Brears H, et al. Multi-organ impairment and long COVID: a 1-year prospective, longitudinal cohort study. J R Soc Med. 2023;116:97–112.

[22] Welikala RA, Fajtl J, Johnson G, Rahman F, Podoleanu R, Remagnino P, Freeman EE, Chambers R, Bolter L, Anderson J, et al. Artificial intelligence-enabled retinal vasculometry at scale utilizing the UK Biobank, CLSA, and NEL DESP datasets. In: 2024 IEEE EMBS International Conference on Biomedical and Health Informatics (BHI). IEEE; 2024:1–8. [Abstract]

[23] Quigley HA, Brown AE, Morrison JD, Drance SM. The size and shape of the optic disc in normal human eyes. Arch Ophthalmol. 1990;108:51–57.

[24] van der Meer RW, Diamant M, Westenberg JJ, Doornbos J, Bax JJ, de Roos A, Lamb HJ. Magnetic resonance assessment of aortic pulse wave velocity, aortic distensibility, and cardiac function in uncomplicated type 2 diabetes mellitus. J Cardiovasc Magn Reson. 2007;9:645–651.

[25] Shakespeare R, Rudnicka AR, Welikala R, Barman SA, Khawaja AP, Foster PJ, Owen CG. Retinal vasculometry associations with cognition status in UK Biobank. Alzheimers Dement. 2025;17:e270087.

[26] Ferreira VM, Schulz-Menger J, Holmvang G, Kramer CM, Carbone I, Sechtem U, Kindermann I, Gutberlet M, Cooper LT, Liu P, et al. Cardiovascular magnetic resonance in nonischemic myocardial inflammation: expert recommendations. J Am Coll Cardiol. 2018;72:3158–3176.

[27] Hirose K, Nakanishi K, Daimon M, Sawada N, Konoma S, Kobayashi S, Seki H, Yoshida Y, Hirokawa M, Nakao T, et al. Association of PREVENT risk model with body fat distribution and subclinical left ventricular dysfunction. Am J Prev Cardiol. 2025;25:101368.

[28] Abhayaratna WP, Seward JB, Appleton CP, Douglas PS, Oh JK, Tajik AJ, Tsang TSM. Left atrial size: physiologic determinants and clinical applications. J Am Coll Cardiol. 2006;47:2357–2363.

[29] Moura B, Aimo A, Al-Mohammad A, Flammer A, Barberis V, Bayes-Genis A, Brunner-La Rocca HP, Fontes-Carvalho R, Grapsa J, Hülsmann M, et al. Integration of imaging and circulating biomarkers in heart failure: a consensus document by the Biomarkers and Imaging Study Groups of the Heart Failure Association of the European Society of Cardiology. Eur J Heart Fail. 2021;23:1577–1596.

[30] O'Neil A, Welikala RA, Barman SA, Owen CG, Rudnicka AR, Rakesh M, Roy-Gagnon MH, Maberley D, Freeman EE. Factors associated with retinal vessel traits in the Canadian Longitudinal Study on Aging. Invest Ophthalmol Vis Sci. 2025;66:13.

[31] Ikram MK, Cheung CY, Lorenzi M, Klein R, Jones TL, Wong TY. Retinal vascular calibre as a biomarker for diabetes microvascular complications. Diabetes Care. 2013;36:750–759.

[32] Ortín Vela S, Bergmann S. Cross-organ analysis reveals associations between vascular properties of the retina, the carotid and aortic arteries, and the brain. Commun Med. 2026;6:102.

[33] Mitchell GF, Vita JA, Larson MG, Parise H, Keyes MJ, Warner E, Vasan RS, Levy D, Benjamin EJ. Cross-sectional relations of peripheral microvascular function, cardiovascular

disease risk factors, and aortic stiffness: the Framingham Heart Study. Circulation. 2005;112:3722–3728.

[34] Tapp RJ, Owen CG, Barman SA, Strachan DP, Welikala RA, Foster PJ, Whincup PH, Rudnicka AR. Retinal microvascular associations with cardiometabolic risk factors differ by diabetes status: results from the UK Biobank. Diabetologia. 2022;65:1652–1663.

[35] Ramesh P, Yeo JL, Brady EM, McCann GP. Role of inflammation in diabetic cardiomyopathy. Ther Adv Endocrinol Metab. 2022;13:20420188221083530..

[36] Sun C, Wang JJ, Mackey DA, Wong TY. Retinal vascular calibre: systemic, environmental, and genetic associations. Surv Ophthalmol. 2009;54:74–95.

[37] Raisi-Estabragh Z, Jaggi A, Gkontra P, McCracken C, Aung N, Munroe PB, Neubauer S, Harvey NC, Lekadir K, Petersen SE. Cardiac magnetic resonance radiomics reveal differential impact of sex, age, and vascular risk factors on cardiac structure and myocardial tissue. Front Cardiovasc Med. 2021;8:763361.

[38] Bilak JM, Alam U, Miller CA, McCann GP, Arnold JR, Kanagala P. Microvascular dysfunction in heart failure with preserved ejection fraction: pathophysiology, assessment, prevalence and prognosis. Card Fail Rev. 2022;8:e24.

[39] Ashokprabhu ND, Quesada O, Alvarez YR, Henry TD. INOCA/ANOCA: mechanisms and novel treatments. Am Heart J Plus. 2023;30:100302.

[40] McDonagh TA, Metra M, Adamo M, Gardner RS, Baumbach A, Böhm M, Burri H, Butler J, Čelutkienė J, Chioncel O, et al. 2023 focused update of the 2021 ESC guidelines for the diagnosis and treatment of acute and chronic heart failure: Developed by the task force for the diagnosis and treatment of acute and chronic heart failure of the European Society of

Cardiology (ESC) With the special contribution of the Heart Failure Association (HFS) of the ESC. Eur Heart J. 2023;44:3627–3639.

[41] Zhan Y, Friedrich MG, Dendukuri N, Lu Y, Chetrit M, Schiller I, Joseph L, Shaw JL, Chuang ML, Riffel JH, et al. Meta-analysis of normal reference values for right and left ventricular quantification by cardiovascular magnetic resonance. Circ Cardiovasc Imaging. 2024;17:e016090.

[42] Kawel-Boehm N, Hetzel SJ, Ambale-Venkatesh B, Captur G, Francois CJ, Jerosch-Herold M, Salerno M, Teague SD, Valsangiacomo-Buechel E, van der Geest RJ, et al. Reference ranges ("normal values") for cardiovascular magnetic resonance (CMR) in adults and children: 2020 update. J Cardiovasc Magn Reson. 2020;22:87.

[43] Roca-Fernandez A, Wamil M, Telford A, Carapella V, Borlotti A, Monteiro D, Thomaides-Brears H, Kelly M, Dennis A, Banerjee R, et al. Cardiac abnormalities in long COVID 1-year post-SARS-CoV-2 infection. Open Heart. 2023;10:e002241.

[44] Dennis A, Wamil M, Alberts J, Oben J, Cuthbertson DJ, Wootton D, Crooks M, Gabbay M, Brady M, Hishmeh L, et al. Multiorgan impairment in low-risk individuals with post-COVID-19 syndrome: a prospective, community-based study. BMJ Open. 2021;11:e048391.